Early human brain development

Keunen, Kristin; van der Burgh, Hannelore K; de Reus, Marcel A; Schmidt, Ruben; de Lange, Siemon C; de Vries, Linda S; Benders, Manon J; van den Heuvel, Martijn P

published in
Pediatric Research
2018

DOI (link to publisher)
10.1038/s41390-018-0138-1

document version
Publisher's PDF, also known as Version of record

Pediatric RESEARCH

www.nature.com/pr

CLINICAL RESEARCH ARTICLE

Early human brain development: insights into macroscale connectome wiring

Kristin Keunen[1], Hannelore K. van der Burgh[2], Marcel A. de Reus[3], Pim Moeskops[4], Ruben Schmidt[2], Lisanne J. Stolwijk[1], Siemon C. de Lange[3], Ivana Išgum[4], Linda S. de Vries[1], Manon J. Benders[1] and Martijn P. van den Heuvel[3]

BACKGROUND: Early brain development is closely dictated by distinct neurobiological principles. Here, we aimed to map early trajectories of structural brain wiring in the neonatal brain.

METHODS: We investigated structural connectome development in 44 newborns, including 23 preterm infants and 21 full-term neonates scanned between 29 and 45 postmenstrual weeks. Diffusion-weighted imaging data were combined with cortical segmentations derived from T2 data to construct neonatal connectome maps.

RESULTS: Projection fibers interconnecting primary cortices and deep gray matter structures were noted to mature faster than connections between higher-order association cortices (fractional anisotropy (FA) $F = 58.9$, $p < 0.001$, radial diffusivity (RD) $F = 28.8$, $p < 0.001$). Neonatal FA-values resembled adult FA-values more than RD, while RD approximated the adult brain faster ($F = 358.4$, $p < 0.001$). Maturational trajectories of RD in neonatal white matter pathways revealed substantial overlap with what is known about the sequence of subcortical white matter myelination from histopathological mappings as recorded by early neuroanatomists (mean RD 68 regions $r = 0.45$, $p = 0.008$).

CONCLUSION: Employing postnatal neuroimaging we reveal that early maturational trajectories of white matter pathways display discriminative developmental features of the neonatal brain network. These findings provide valuable insight into the early stages of structural connectome development.

Pediatric Research (2018) 84:829–836; https://doi.org/10.1038/s41390-018-0138-1

INTRODUCTION

Human gestation marks the onset of comprehensive development of the human brain. Fundamental processes of brain development including neurogenesis, neuronal migration, synaptogenesis, and axonal pathfinding take place during the earliest gestational phases, i.e., from the fetal period commencing at eight postconceptional weeks continuing through the early postnatal period.[1–3] By the time of term birth, all major white matter pathways are in place[4,5] and the neonatal cortex approximates the shape of the adult human brain.[3,6]

Diffusion-weighted imaging (DWI) studies in postmortem fetal brains have identified axonal projections from as early as 13 weeks postconceptional age.[4,7] Major white matter pathways develop in a hierarchical order, predominantly during the second trimester of pregnancy, with limbic tracts and thalamocortical projection fibers emerging first, followed by commissural tracts that interconnect both hemispheres and intrahemispheric association pathways originating last.[5,7] Structural connectome studies in preterm infants have revealed an adult-like connectivity framework as early as 27 weeks gestational age.[8–10] By this time, pivotal brain network attributes are already present, including short communication paths favoring efficiency, clustering of brain regions for specialized information processing, and a central core of brain hubs, reflecting brain regions that are connected to a large number of other brain regions and therefore play a crucial role in communication facilitation, referred to as the rich club.[8–11]

To date, developmental trajectories of the earliest stages of macroscale brain network development remain largely unexplored. Here, we aimed to further our understanding of early structural connectome development of the neonatal brain during the earliest phases that allow postnatal in vivo neuroimaging, i.e., during the developmental period that coincides with the last trimester of pregnancy. Furthermore, we set out to investigate how these developmental changes relate to what is known about their underlying neurobiology. In addition, we aimed to make direct comparisons of early structural changes in the neonatal brain and structural connectivity in the adult human brain. To this end, we derived structural connectivity matrices from DWI scans and T2-weighted images acquired in 44 newborn infants (23 preterm and 21 full-term infants) scanned shortly after birth between 29 and 45 weeks postmenstrual age. We hypothesized that thalamocortical projection fibers interconnecting deep gray matter structures and primary cortices (i.e., primary sensory and motor areas) would follow different maturational trajectories than association fibers between heteromodal association cortices (i.e., cortical regions governing higher cognitive functions and involved in integration of information from sensory and decision-making brain regions) well before they are myelinated. Given the sequence of emergence of these fibers,[4,5,7] we hypothesized that

[1]Department of Neonatology, Wilhelmina Children's Hospital, University Medical Center Utrecht and Utrecht University, Utrecht, Netherlands; [2]Department of Neurology, University Medical Center Utrecht and Utrecht University, Utrecht, Netherlands; [3]Department of Psychiatry, University Medical Center Utrecht and Utrecht University, Utrecht, Netherlands and [4]Image Sciences Institute, University Medical Center Utrecht and Utrecht University, Utrecht, Netherlands
Correspondence: Martijn Heuvel (m.p.vandenheuvel@umcutrecht.nl)

Received: 23 October 2017 Revised: 16 July 2018 Accepted: 18 July 2018
Published online: 15 August 2018

their maturational trajectories would follow a similar developmental pattern. In addition, we compared early developmental changes in white matter diffusion properties against historical mappings of subcortical myelination as performed by pioneering neuroanatomists in the early to mid 1900s.[12,13] As a secondary objective, we studied whether brain network attributes crucial for human brain functioning exhibit early developmental changes and explored their association with measures of cognitive functioning in infancy. Third, we aimed to investigate the resemblance of the neonatal brain network to the adult connectome.

METHODS

Study population

In this study, we set out to investigate typical macroscale connectome development in the earliest phases of human development that allow in vivo delineation of these processes. Because of ethical restrictions, we were not able to include healthy fetuses or healthy full-term infants. We therefore aimed to approximate typical brain development by selecting infants who underwent neuroimaging for clinical reasons but that did not display overt brain injury. Infants eligible for participation in this study had been admitted to the level III or level II Neonatal Intensive Care Unit of the Wilhelmina Children's Hospital, University Medical Center Utrecht, Netherlands between June 2013 and June 2015. Infants were included in this prospective cross-sectional observational study if the following criteria were met: (1) no focal brain injury, (2) no genetic syndrome, congenital infection of the central nervous system, or inborn error of metabolism, (3) good quality MRI data including T2-weighted imaging, DWI and resting-state-functional MRI (not reported here), and (4) an MRI acquisition as soon as clinically feasible after birth in order to minimize the likelihood of introducing—potentially detrimental—effects of the extra-uterine environment on the developing brain. Based on these criteria, 47 infants were eligible for inclusion in this study. Processing of the MRI data failed in three subjects owing to suboptimal cortical parcellations (described in the section on brain tissue segmentation and connectome reconstruction). The final cohort therefore comprised 44 neonates.

Neurodevelopmental outcome was formally evaluated at 18 months corrected age using the Griffiths Mental Development Scales and/or at 24 months corrected age using the Bayley Scales of Infant and Toddler Development, Third Edition (BSITD-III)[14] in 34 (77%) infants (20 preterm and 14 full-term). The BSITD-III assessment could not be completed in one other child because of hospital-related anxiety. The development quotient at age 12 months was 96 in this child. Neurodevelopmental follow-up was not indicated in the remaining nine infants at the discretion of the attending physician. The majority of infants ($n = 27$, 79%, [16 preterm and 11 full-term]) had cognitive outcome scores within the normal range, defined as one standard deviation from the normative mean (normative mean BSITD-III 100 ± 15 and Griffiths Mental Development Scales[15] 100 ± 12, mean in this population 103 ± 12). The remaining seven infants had either higher cognitive scores (119, 120, 120, and 129 [three preterm and one full-term]) or lower cognitive composite scores. The three children (two full-term and one preterm) scoring below the normal range had a cognitive composite score of 82 and motor composite scores of 95, 115, and 118 on the BSITD-III. Cognitive scores on the Griffiths Mental Development Scales were computed by taking the average of the personal-social, hearing and language, and performance subscales.

The Institutional Review Board of the University Medical Center Utrecht, Netherlands (IRB) gave approval for use of the clinically acquired data for scientific examinations as conducted in this study. Since we only made use of clinically obtained data, written informed parental consent for participation in the study was waived by the IRB. Clinical characteristics of the study population are outlined in Table 1.

MRI procedure

All scans were acquired on a 3-tesla Philips Achieva clinical scanner (Philips Healthcare, Best, Netherlands). Details about the MRI procedure are described in the Supplemental Materials.

Brain tissue segmentation and connectome reconstruction

T2-weighted images were automatically segmented into eight tissue classes. The segmentation process is depicted in the Supplemental Materials and a detailed description of the segmentation algorithm is provided by Moeskops et al.[16] Next, the cortical mantle of each individual subject was reconstructed and parcellated into 68 distinct anatomical brain regions (34 per hemisphere) and 14 deep gray matter regions (seven per hemisphere) with the Freesurfer image analysis suite (V5, http://surfer.nmr.mgh.harvard.edu).[17] The Freesurfer registration algorithm is based on curvature information. Parcels were thus based on similar anatomical landmarks across all subjects, rendering the parcellation highly comparable between subjects.[18] Prior to the automated Freesurfer process, surrogate T1-weighted images were reconstructed from the brain tissue segmentations by assigning tissue intensity values to each tissue class in the neonatal segmentation that correspond with expected adult T1-weighted signal intensity. Hence, brain tissue segmentations now displayed similar tissue contrast as adult T1-weighted images,

Table 1. Characteristics of the study population

	Very preterm infants (<32 weeks) n=17	Late preterm infants (32–36 weeks) n=6	Full-term infants n=21
Gestational age (weeks)	27.4 (26.1–31.9)	33.4 (32.0–36.7)	40.0 (37.0–41.6)
Birth weight (g)	1145 (590–2050)	1808 (1205–4300)	3296 ± 636
Sex (female)	9 (53%)	1 (17%)	12 (57%)
Postmenstrual age MRI (weeks)	31.0 (29.7–34.7)	35.1 (34.1–38.4)	41.4 ± 1.8
Postnatal age MRI (days)	23 ± 8	9 (5–23)	9 (2–31)
Neurodevelopmental outcome[a]	108 (82–121)	115 (91–129)	101 (82–120)
Age at outcome assessment (months)	20.5 (17.4–28.9)	24.9 (17.5–26)	24.1 (17.6–24.8)

Data are displayed as mean, standard deviation (±) for normally distributed data and median, range for non-normally distributed data
[a]Neurodevelopmental outcome was defined as a composite of either the cognitive composite score extracted from the Bayley Scales of Infant and Toddler Development, Third Edition ($n = 25$) performed at age 24 months or a composite of the personal-social, hearing and language, and performance subscales on the Griffiths Mental Development Scales at age 18 months ($n = 9$). Follow-up data were not available for 10 infants (see Methods section)

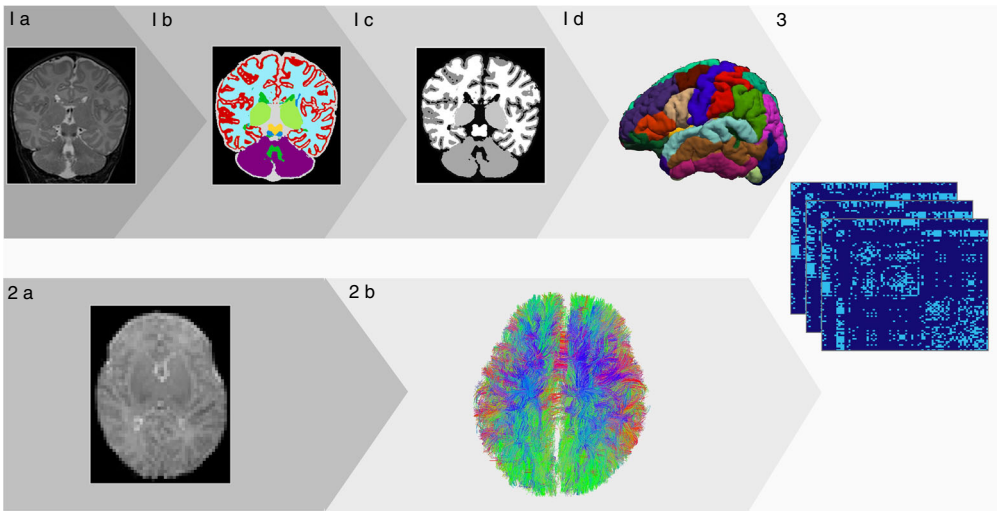

Fig. 1 Overview of the pipeline for neonatal connectome reconstruction 1a. T2-weighted images acquired in the coronal plane are segmented into distinct tissue types including cortical gray matter, unmyelinated white matter, cerebellum, deep nuclear gray matter and cerebrospinal fluid[16] as illustrated in 1b. Next, surrogate "T1-weighted" images are created by assigning similar brain tissue intensity to the brain tissue segmentations as adult T1-weighted images (1c). Parcellation of the cortical mantle is performed employing the Freesurfer image analysis suite[17] using these surrogate T1-weighted images as input (1d). Diffusion-weighted images (DWI images) are realigned to the $b = 0$ image (2a), corrected for small head movements and EPI distortion. Next, DWI images are automatically registered to the segmentation results from Freesurfer and manually adjusted when appropriate (2b). Whole-brain streamline tractography is performed with the following settings: FA 0.01, maximum angle 45°, 27 seeds per voxel and a minimum fiber length of 8 mm * 3^√ (factor intracranial volume) (see Supplemental Materials for detailed description). Streamlines are terminated when they leave the white matter mask. (3) Finally, whole-brain streamline tractography results and the results from the cortical parcellation are collated, resulting in connectivity matrices of 82×82 regions, including 68×68 cortical regions as defined by the Desikan–Killiany atlas[26]

which is a prerequisite for the analysis with Freesurfer (Fig. 1). The first step of the Freesurfer reconstruction pipeline was adapted as such that resampling was performed using a nearest neighbor approach, instead of linear interpolation (default).

Preprocessing of the DWI data included the following steps: first, data quality of each subject's DWI dataset was visually inspected. DWI images were corrected for eddy-current distortions and small head movements.[19] Secondly, they were realigned to the $b = 0$ image and third, a tensor was fitted to the diffusion signal within each voxel using a robust tensor fitting algorithm (RESTORE).[20] DWI data were registered to the parcellation results using the tkregister tool in FreeSurfer. Registration results were visually inspected and manually optimized. Next, deterministic streamline tractography was performed to reconstruct the structural connectome of each infant. Details about the procedure are outlined in the Supplemental Materials. The complete processing pipeline of neonatal structural connectome reconstruction is outlined in Fig. 1.

Data analyses were performed on binary and weighted connectivity matrices (FA and radial diffusivity [RD] in mm^2/s). These matrices were obtained using two distinct procedures, both based on consistency of white matter paths across subjects (consensus masking). First, individual weighted matrices were computed employing a number of streamlines (NOS)-threshold ≥3 streamlines. This streamline threshold was set in order to account for false positives.[21] The weights in the connectivity matrices consisted of FA and RD and these were selected as primary variables of interest because they were previously reported to exhibit relevant developmental changes during the timeframe of our study.[9,22,23] In detail, the NOS-thresholded connectivity map was laid over the weighted connectivity matrices as a brain mask, leading to connections being included if they comprised ≥3 streamlines. Connections comprising <3 streamlines were considered absent and therefore set to zero. Connectivity matrices were binarized by setting the positive weights (i.e., weights > 0) in the acquired weighted connectivity matrices to one. Binary connectivity matrices were used in the analyses comparing the adult brain to the neonatal connectome (see section "Resemblance to the adult connectome").

Secondly, consensus masking was performed using the prevalence across subjects. To this end, subjects were sorted by postmenstrual age at time of scan and subdivided into groups of five individual infants. A sliding window was used with steps of two subsequent subjects and a subgroup prevalence of 60%;[24] i.e., connections were included when they were present in at least three out of five infants within a specific subgroup. In this way, weighted (FA and RD weighted) connectivity maps were acquired.

Connection-wise analyses

We zoomed in on developmental trajectories of specific groups of edges, focusing on primary and heteromodal association fibers. Primary connections were defined as white matter pathways interconnecting the subcortical gray matter and precentral gyrus (i.e., primary motor cortex), postcentral gyrus (i.e., somatosensory cortex), and pericalcarine cortex (i.e., primary visual cortex). Heteromodal association fibers were defined as connections between the frontal cortex including the superior–frontal cortex, rostral–middle frontal cortex, pars opercularis, pars triangularis and pars orbitalis, the superior–parietal cortex, supramarginal gyrus, precuneus, anterior–cingulate cortex, and middle temporal gyrus. FA and RD of these connections were calculated on individual connectome maps.

Flechsig atlas

In the early 1900s, neuroanatomist Paul Flechsig published his findings on "medullary substance" expansion in the postnatal subcortical white matter.[12] His atlas that divided the cortex into specific areas based on their sequence of subcortical myelination was modified by Von Bonin in the 1950s.[13] Here, we adopted the modified Flechsig and Von Bonin atlas as reported previously.[25] Regions were manually mapped to the DK atlas[17,26] employing a winner-takes-it-all approach: the myelination number as provided

by Flechsig and Von Bonin that comprised the greatest surface area of the cortical region as defined by the DK atlas was assigned to that specific brain region for each of the 68 cortical areas.

Graph theory

Network metrics were calculated on individual weighted connectome maps using the Brain Connectivity Toolbox.[27] Connectome maps consisting of 82 brain regions (including 14 subcortical regions) were entered in these analyses. The following network metrics were included in the analyses: network density, weighted normalized global efficiency, the weighted normalized clustering coefficient, and modularity. Network metrics used in this study are depicted in the Supplemental Materials.

Resemblance to the adult connectome

In order to investigate the overlap between the neonatal brain network and the adult human connectome and validate findings from our previous report on the neonatal connectome in a different sample,[9] we compared neonatal networks against connectome maps derived from high-quality DWI data from 487 adult subjects (males and females, aged 22–35 years) as provided by the 500 Subjects Release from the Human Connectome Project.[28] Details about the process of adult connectome reconstruction as well as the comparison analyses are listed in the Supplemental Materials.

Experimental design and statistical analysis

This study is a prospective observational cohort study. In what follows, we will describe the statistical analyses used in our study. Means and standard deviations were reported for normally distributed data. Data that were not normally distributed were reported as median and their corresponding range. The relationship between postmenstrual age and brain connectivity measures, including white matter diffusion properties (FA and RD) or primary and association fibers, higher-order brain network metrics, and resemblance parameters between the neonatal brain and adult connectome was investigated using Pearson correlations for linear relationships and Spearman rank correlations for non-linear relationships. The significance level (two-sided p-value) was set to an alpha of 0.05 in all analyses, unless otherwise specified.

Network density increased substantially with age ($r = 0.83$, $p < 0.001$). Therefore, a number of approaches were used to account for its potential effect on higher-order network metrics[29] (i.e., normalized global efficiency, modularity, and normalized clustering in our study). First, network cost (i.e., density) was added as a covariate to a general linear model investigating the association between postmenstrual age (independent variable) and relevant network metrics (dependent variable). Conversely, density was selected as the variable of interest (i.e., dependent variable) and postmenstrual age and relevant network metrics were entered as independent variables. Second, a prevalence threshold was employed and set as follows. The prevalence of connections was calculated in the youngest age group. Next, the lowest prevalence threshold was chosen at which density was not significantly correlated with postmenstrual age. The group mask formed based on this threshold was applied to the connectivity matrices of all infants.

Mean FA and RD of primary and higher-order association connections were compared using paired t-tests. The effect of postmenstrual age was analyzed using ANCOVA. Post hoc paired samples t-tests were performed when the ANCOVA yielded significant results employing a Bonferroni correction for statistical significance. p-values less than .025 (i.e. 0.05/2) were thus considered statistically significant.

The relationship between white matter maturation and subcortical myelination order as provided by Flechsig and Von Bonin was investigated as follows. First, node-wise FA and RD were calculated (1) by taking the mean of their non-zeros components and (2) by taking the sum of their components (i.e., calculated node strength). The latter analysis was included to take differences in node degree into account. These metrics were computed on connectome maps of age-consecutive subgroups. Second, node-wise alterations in FA and RD were calculated, defined as the difference in node-wise mean FA and RD between the youngest ($n = 5$) and most mature subgroup ($n = 5$). Subgroups were extended to $n = 10$ youngest and most mature infants. Node-wise changes were related to Flechsig mappings using a Spearman rank correlation.

Alterations of the relative difference in RD, axial diffusivity (AD) and FA between the neonatal white matter of individual subjects and the adult brain over the 16 weeks time-period were analyzed using ANCOVA entering postmenstrual age as a covariate and employing a post hoc Bonferroni correction. Additionally, a general linear model was performed for each metric to estimate its slope.

RESULTS

Primary and heteromodal association fibers

First, we investigated whether thalamocortical projection fibers between deep gray matter structures and primary cortices displayed divergent trajectories from association fibers interconnecting higher-order cortices. To this end, we compared FA and RD as measures of white matter microstructural maturation between these fiber categories over the 16-week developmental period. FA of primary connections was significantly higher than FA of heteromodal association fibers ($t(43) = 5.9$, $p < 0.001$, paired t-test) and increased significantly faster with postmenstrual age ($F(1,84) = 58.9$, $p < 0.001$, ANCOVA). Conversely, RD of primary connections was significantly lower ($t(43) = -9.0$, $p < 0.001$) and decreased significantly faster than RD of higher-order association fibers $F(1,84) = 28.8$, $p < 0.001$). Results are outlined in Fig. 2. In order to account for the difference in number of connections, with heteromodal association fibers being larger in number than primary connections, analyses were repeated on random selections of an equal number of primary and heteromodal association connections. These analyses yielded similar results (Supplemental Materials).

Flechsig mappings

Next, region-wise alterations in RD and FA were compared against what is known about the sequence of subcortical myelination from postmortem examinations as performed by early neuroanatomists. Differences in RD between the youngest and most mature neonatal subgroup were correlated with Flechsig mappings of subcortical myelination (mean RD Spearman rank $r = 0.45$, $p = 0.008$, sum RD $r = 0.50$, $p = 0.002$). Results of the correlation between mean RD and subcortical myelination as provided by Flechsig and Von Bonin are portrayed in Fig. 3. Similar results were found when extending the age groups to $n = 10$ youngest and $n = 10$ most mature infants (mean RD $r = 0.45$, $p = 0.008$, sum RD $r = 0.47$, $p = 0.005$). Correlations of mean and cumulative node-wise FA were not significantly related to Flechsig mappings.

Network metrics

Third, we investigated the developmental trajectories of the structural connectivity framework in the neonatal brain between 29 and 45 weeks PMA. Normalized global efficiency of FA-weighted brain networks significantly increased with advancing postmenstrual age (Pearson $r = 0.38$, $p = 0.01$). Results are displayed in Fig. 4. Modularity and normalized clustering did not significantly change over the 16 weeks study period. Furthermore, RD-weighted network metrics did not significantly change with increasing postmenstrual age.

To explore the effect of density on the association between postmenstrual age and normalized global efficiency, density was

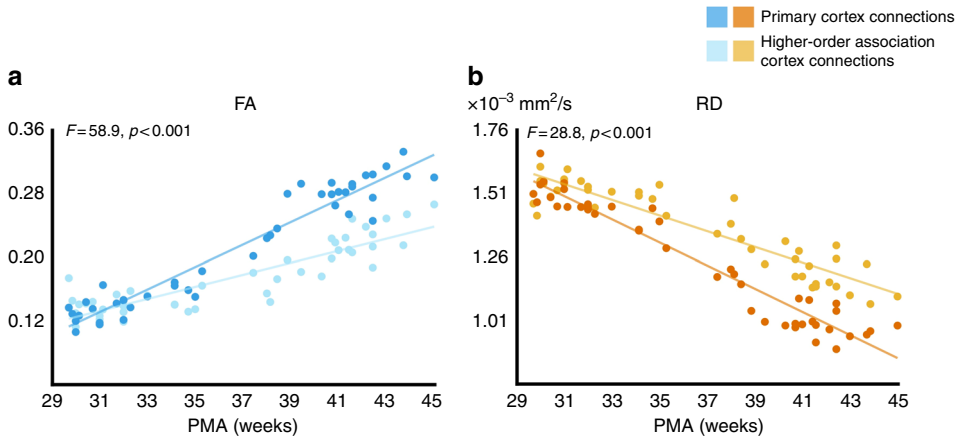

Fig. 2 Maturational trajectories of primary and heteromodal association fibers. Alterations in mean FA (left panel) and mean RD (right panel) with postmenstrual age are outlined. Primary connections are depicted in bright colors and reveal significantly faster trajectories. Multimodal connections are illustrated in pale colors

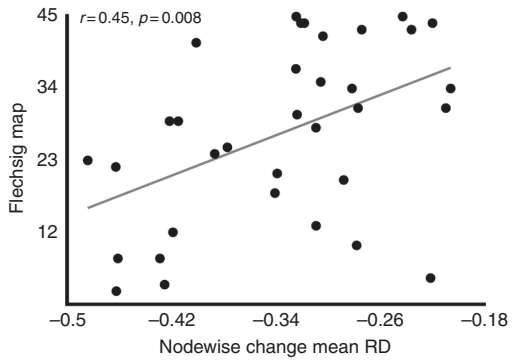

Fig. 3 RD changes related to historical Flechsig mappings. Scatter plot outlines the correlation between changes in RD and histopathological recordings of subcortical myelination as performed by Flechsig in the early 1900s and modified by Von Bonin in the 1950s. Cortical regions showing the greatest early change in RD were significantly correlated to the sequence of subcortical myelination as provided in the modified Flechsig atlas. Change in RD was defined as the difference in mean RD between the youngest and most mature subgroup for each region, averaged over the two hemispheres

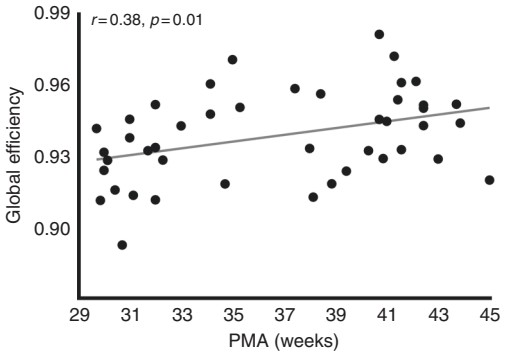

Fig. 4 Early developmental changes in global efficiency of the neonatal brain network. Alterations in global efficiency over 16 developmental weeks that reflect the third trimester of normal pregnancy and first postnatal weeks are illustrated. Normalized global efficiency increased significantly with postmenstrual age as measured on FA-weighted connectome maps

added as a covariate to a general linear model investigating their relationship. The model was statistically significant ($F(1,41) = 3.64$, $p = 0.04$). There was no significant interaction between density and postmenstrual age ($t = -0.006$, $p = 0.995$). Next, the association between postmenstrual age and density was examined; entering normalized global efficiency as a covariate in the model in order to further explore their interchangeability. The model was statistically significant ($F(1,41) = 41.1$, $p < 0.0001$) and postmenstrual age was the major contributor to the model ($t = 8.2$, $p < .0001$), while normalized global efficiency did not add significantly ($t = 0.6$, $p = 0.57$). Subsequently, a prevalence threshold was employed based on the presence of connections in 80% of subjects in the youngest age group. Normalized global efficiency was not significantly correlated with postmenstrual age ($r = 0.29$, $p = 0.06$) (Supplemental Fig. 1). Network metrics were not significantly correlated with early cognitive functioning as measured at age 18–24 months.

Resemblance adult connectome

The relative difference in diffusion properties between neonates and adults was smallest for FA and largest for RD. The relative distance of FA in the neonatal brain to FA in the adult brain varied between −0.73 and −0.68 at the earliest time-points (29–30 weeks PMA) and decreased to −0.52 through −0.44 by 42–45 weeks PMA. RD was 2.11–2.45 times higher in the youngest infants than RD in the adult brain and declined to 1.37–1.67 times higher values in the most mature group of infants. Distilling the components attributing to FA, the relative difference in AD between the neonatal brain and adult brain decreased least (Fig. 5a). The relative difference in RD, AD, and FA was significantly different between the groups (ANCOVA $F(1,126) = 358.4$, $p < 0.001$) and the relative difference in RD declined fastest with postmenstrual age (coefficient RD −0.046 versus FA 0.041, AD 0.005).

The modified Mantel test (see Supplemental Materials for a detailed description) revealed that the binary connectome showed substantial overlap with the adult brain network (>0.80 at all developmental time-points) thereby reconfirming findings from our previous report on the neonatal brain network in a different neonatal sample.[9] Similarities between the neonatal and adult connectome increased moderately with postmenstrual age (Pearson $r = 0.58$, $p < 0.001$) (Fig. 5b).

DISCUSSION

Combining data from DWI and T2-weighted imaging in 44 newborn infants, we provide insight into early white matter

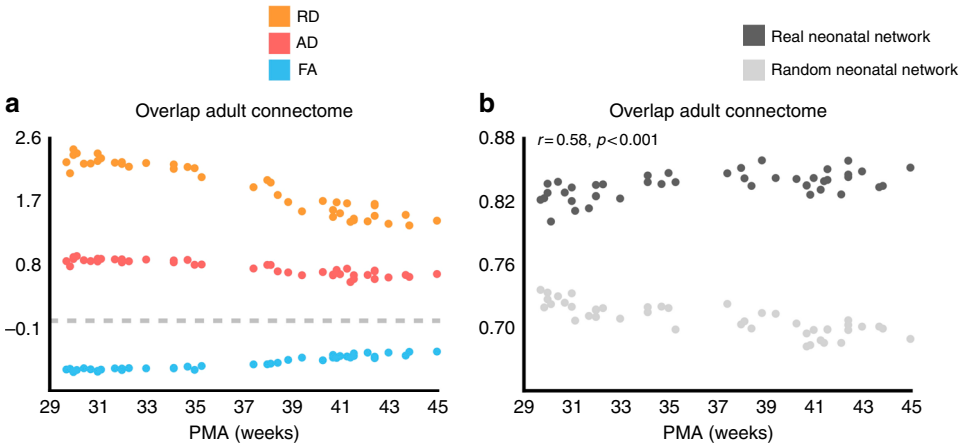

Fig. 5 Differences and similarities between neonates and adults. Relative differences in FA (blue), AD (reddish-pink), and RD (orange) are portrayed in **a**. Dotted gray line indicates adult level (i.e., no difference). The relative difference between neonates and adults is smallest in FA, while RD differences decrease at a faster pace (beta-coefficient RD −0.07 versus FA 0.02). Panel **b** illustrates the results of the modified Mantel test (see Supplemental Materials), which revealed substantial overlap of the neonatal connectome and the adult human brain network. Similarity exceeded 0.80 at all time-points and increased gradually with postmenstrual age

development between 29 and 45 weeks postmenstrual age in vivo, revealing distinct early developmental features. Development of premyelinated primary projection fibers preceded maturation of heteromodal association fibers. In addition, early white matter changes in RD were significantly correlated with histopathological mappings of subcortical myelination as performed by early neuroanatomists.[12,13] FA did not show such correlations, yet verged on the adult human brain most. Collectively, these findings provide evidence that diffusion properties feature distinct developmental trajectories, with FA approximating the adult brain and RD reflecting an early marker of subcortical white matter myelination. Consequently, these early developmental trajectories may delineate valuable parameters of typical perinatal white matter development and may therefore assist in the designation of deviances thereof.

Using clinically applicable DWI, we were able to reconfirm the well-documented maturational trajectories of white matter fibers, which have been established through elaborate research efforts on postmortem brain tissue employing both histopathological examinations and high-resolution diffusion imaging techniques.[4,5,7,22,23] Limbic and projection fibers are known to originate first, followed by commissural fibers of the corpus callosum and association fibers deriving last.[1,5,7] Nearly a century ago, pioneering neuroanatomists mapped the sequence of subcortical myelination and outlined their concept of the neurobiological principles that orchestrate this developmental process.[12,30] These rules correspond substantially to the order of white matter tract formation, with projection fibers myelinating before association tracts. Here, we demonstrate primary connections to exhibit a faster maturational course than multimodal association fibers from as early as ~32 weeks PMA onwards. In addition, we reveal that early maturational changes in RD, which are present well before fibers are myelinated correspond to the sequence of myelination as mapped in postmortem histopathological recordings of peri- and postnatal myelination.[12,30,31] Conversely, FA did not show such correlation.

The notion that RD and FA depict distinct maturational features is in agreement with previous DWI studies and postmortem reports.[23,32,33] Increasing FA has been noted to predominantly reflect progressive fiber coherence, decreasing membrane permeability and myelination, while decreasing RD is thought to result from reductions in brain water content, advancing fiber organization, functional maturation of intracellular compartments including the cytoskeleton and microtubules and increases in membrane density owing to proliferation of maturing oligodendrocytes and subsequent myelination of white matter fibers. RD reductions also coincide with current knowledge about the decline in radial glial fibers, which govern neuronal migration during embryonic and fetal brain development and proliferate to become radial glial cells that support axons when their role in neuronal migration is completed.[23,34] Although our analyses do not allow direct comparisons with their underlying neurobiology, they point toward biologically meaningful divergent trajectories, with RD being an early marker of subsequent myelination and FA —as a reflection of increasing fiber coherence—resembling the adult human brain more. As such, these findings are clinically relevant for the designation of early developmental white matter changes that may occur as a consequence of perinatal brain injury, preterm birth, or congenital heart disease.[35–37]

We observed a significant increase in global efficiency of FA-weighted networks with advancing postmenstrual age. The observation of a neonatal brain network that increasingly supports global communication consolidates previous findings on structural connectivity in preterm infants.[8,9,22] However, its interpretation is not straightforward. Network cost (density) was found to similarly increase with postmenstrual age and the latter measure is known to substantially influence network metrics describing the brain's topology, including global efficiency.[29] Here, we aimed to control for density changes using normalization, additionally employing a prevalence threshold and interchanging density and global efficiency as a covariate in the statistical model. These analyses confirmed the hypothesis that residual impact of network cost cannot be precluded after normalization of network metrics, if density differences are present in a study population. The multivariable regression analysis of postmenstrual age and density revealed that normalized global efficiency did not significantly contribute to the model. Furthermore, postmenstrual age was not significantly correlated with normalized global efficiency using a prevalence threshold.

To date, studies investigating early developmental trajectories of structural brain network organization remain scarce, but the few earlier reports that we are aware of consistently demonstrated decreasing path length between ~30 weeks postmenstrual age and term age, denoting increasing integration capacity.[8,9,22] Concomitantly, these studies uncovered density changes with age.[8,22] Similar to our study, Ball et al.[8] used diffusion tensor imaging and demonstrated increasing density with advancing age during a developmental period that coincides with the timeframe of our study. Notably, Batalle and colleagues[22] reported decreasing density with increasing age employing DWI with multiple

shells, which allowed constrained spherical deconvolution tractography. Together, these findings stress the complexity of the concept of density and that inferences about the implied formation of novel fibers cannot be drawn from diffusion tensor imaging in vivo alone.

Consequently, the clinical DWI protocol that we used in our study is a limitation. The tradeoff between state-of-the-art DWI imaging and clinical feasibility including limited scan time and the infant's comfort, which naturally comes first, resulted in the decision to use this clinical DWI protocol which lasted little over 5 min and was successful in all infants included in the study. However, it inherently imparted limitations on the reconstruction of complex fiber orientations (i.e., crossing fibers in single voxels) and resulted in neonatal connectivity matrices of different density. Another important consideration is that we were not able to include healthy fetuses or healthy full-term infants owing to ethical objections by the IRB of our institution at the time the study was designed. We thus aimed to approximate typical brain development by selecting infants who did not exhibit brain injury and were scanned as soon as clinically feasible after birth in case of preterm birth. None of the infants included in the follow-up program ($n = 35$, 80%) showed signs of neurodevelopmental delay on formal assessments in infancy. Regardless, we included preterm infants in our study to obtain estimates of third trimester white and gray matter development and prematurity may have impacted their designated trajectories.[22,38,39] Such effects may have resulted in delayed white matter maturation owing to developmental insults including neonatal illness, malnutrition and the administration of neuro-suppressive drugs, but may have also facilitated maturation because of exposure to sensory stimuli.[5,40,41] A recent resting-state fMRI study revealed functional connectivity reductions to be present in the fetal brain even *before* preterm birth in 14 fetuses that were to be born prematurely.[39] Hence, we cannot rule out that prematurity and its consequences may have affected the relationship between postmenstrual age and white matter maturation in our study. It would thus be of particular interest to repeat the present analyses in healthy fetuses and neonates, granted that methodological hurdles innate in fetal neuroimaging are overcome.

In conclusion, we reveal that premyelinated white matter fibers in the neonatal brain have specific developmental trajectories; with primary connections being strengthened before heteromodal association fibers and FA verging on the adult human brain prior to RD, while RD advanced at a faster pace. Our findings corroborate earlier notions of pioneering neuroanatomists who revealed that connections playing a primary role in brain functioning are favored to mature during early brain development and add that these distinct developmental trajectories can be identified in vivo well before myelination becomes apparent. Collectively, these findings provide valuable insight into developmental trajectories of the human brain network shortly after its genesis and are coherent with the neurobiological principles they adhere to. Future research should focus on functional correlates of these structural neurodevelopmental trajectories and is urged to include healthy fetuses to obtain unobscured estimates of typical brain development.

ACKNOWLEDGEMENTS

We thank Nathalie Claessens, Laura Dix, Nienke Wagenaar, and Lauren Weeke for their assistance in the data collection and Filipe Gervásio Gonçalves Costa for his intellectual input on the content of the manuscript. We also thank Ingrid van Haastert, Corine Koopman, Marian Jongmans, A. Wingens, M. Tanke, Tabitha Koops and Sasja Duijff for their careful neurodevelopmental evaluation of the children included in this study. We are grateful to the MRI technicians for their dedication to good quality imaging data acquisition in our neonates. Data were provided in part by the Human Connectome Project, WU-Minn Consortium (Principal Investigators: David Van Essen and Kamil Ugurbil; 1U54MH091657) funded by the 16 NIH Institutes and Centers that support the NIH Blueprint for Neuroscience Research; and by the McDonnell Center for Systems Neuroscience at Washington University. This work was supported by a grant from the Wilhelmina Children's Hospital Research Fund ("Vrienden van het WKZ") to M.P.v.d.H. and M.J. B. The work of M.P.v.d.H. is supported by a VIDI grant from the Netherlands Organisation for Scientific Research (NWO) (grant number 452-16-015), a Rudolf Magnus Fellowship and an MQ Fellowship.

ADDITIONAL INFORMATION

The online version of this article (https://doi.org/10.1038/s41390-018-0138-1) contains supplementary material, which is available to authorized users.

Competing interests: The authors declare no competing interests.

Publisher's note: Springer Nature remains neutral with regard to jurisdictional claims in published maps and institutional affiliations.

REFERENCES

1. Keunen, K., Counsell, S. J. & Benders, M. J. The emergence of functional architecture during early brain development. *Neuroimage* [Internet] 1–13 (2017). http://linkinghub.elsevier.com/retrieve/pii/S105381191730054X
2. Bystron, I., Blakemore, C. & Rakic, P. Development of the human cerebral cortex: Boulder Committee revisited. *Nat. Rev. Neurosci.* **9**, 110–122 (2008). [Internet].
3. Stiles, J. & Jernigan, T. L. The basics of brain development. *Neuropsychol. Rev.* **20**, 327–348 (2010).
4. Takahashi, E., Folkerth, R. D., Galaburda, A. M. & Grant, P. E. Emerging cerebral connectivity in the human fetal Brain: an MR tractography study. *Cereb. Cortex* **22**, 455–464 (2012).
5. Kostovic, I. & Jovanov-Milosevic, N. The development of cerebral connections during the first 20-45 weeks' gestation. *Semin. Fetal Neonatal Med.* **11**, 415–422 (2006).
6. Striedter, G. F., Srinivasan, S. & Monuki, E. S. Cortical folding: when, where, how, and why? *Annu Rev. Neurosci.* **38**, 150421150146009 (2014).
7. Huang, H. et al. Anatomical characterization of human fetal brain development with diffusion tensor magnetic resonance imaging. *J. Neurosci.* **29**, 4263–4273 (2009).
8. Ball, G. et al. Rich-club organization of the newborn human brain. *Proc. Natl Acad. Sci. USA* **111**, 7456–7461 (2014).
9. van den Heuvel M. P., et al. The neonatal connectome during preterm brain development. *Cereb. Cortex* [Internet] 1–14 (2014). http://www.ncbi.nlm.nih.gov/pubmed/24833018
10. Tymofiyeva, O. et al. A DTI-based template-free cortical connectome study of brain maturation. *PLoS ONE* **8**, 1–10 (2013).
11. van den Heuvel, M. P. & Sporns, O. Rich-club organization of the human connectome. *J. Neurosci.* **31**, 15775–15786 (2011).
12. Flechsig, P. *Anatomie des menschlichen Gehirns und Rückenmarks auf myelogenetischer Grundlage* (Georg Thieme, Leipzig, 1920).
13. Von Bonin, G. *Essay on the Cerebral Cortex*, 1st edn. (Charles C Thomas, Springfield, IL, 1950).
14. Van Baar, A. L., Steenis, L. J. P., Verhoeven, M., Hessen, D. J. *Bayley-III NL, Technische en afname handleiding* (Pearson Clinical, Amsterdam, 2014).
15. Huntley, M. *Griffiths Mental Development Scales - Revised: Birth to 2 Years* (Hogrefe Ltd., Oxford, 1996).
16. Moeskops, P., Viergever, M. A., Mendrik, M., De Vries, L. S., Benders, M. J. N. L. Automatic segmentation of MR brain images with a convolutional neural network. *IEEE Trans. Med. Imaging* **5**, 1–10 (2016).
17. Fischl, B. et al. Automatically parcellating the human cerebral cortex. *Cereb. Cortex* **14**, 11–22 (2004).
18. Cammoun, L. et al. Mapping the human connectome at multiple scales with diffusion spectrum MRI. *J. Neurosci. Methods* **203**, 386–397 (2012).
19. Andersson, J. L. R. & Skare, S. A model-based method for retrospective correction of geometric distortions in diffusion-weighted EPI. *Neuroimage* **16**, 177–199 (2002).
20. Chang, L. C., Jones, D. K. & Pierpaoli, C. RESTORE: robust estimation of tensors by outlier rejection. *Magn. Reson Med* **53**, 1088–1095 (2005).
21. Kim, D. J. et al. Children's intellectual ability is associated with structural network integrity. *Neuroimage* **124**, 550–556 (2016).
22. Batalle D., et al. Early development of structural networks and the impact of prematurity on brain connectivity. *Neuroimage* **149**, 379–392 (2017).

23. Xu, G. et al. Radial coherence of diffusion tractography in the cerebral white matter of the human fetus: Neuroanatomic insights. *Cereb. Cortex* **24**, 579–592 (2014).
24. De Reus, M. A. & Van den Heuvel, M. P. Estimating false positives and negatives in brain networks. *Neuroimage* **70**, 402–409 (2013).
25. Glasser, M. F. & Van Essen, D. C. Mapping human cortical areas in vivo based on myelin content as revealed by T1- and T2-weighted MRI. *J. Neurosci.* **31**, 11597–11616 (2011).
26. Desikan, R. S. et al. An automated labeling system for subdividing the human cerebral cortex on MRI scans into gyral based regions of interest. *Neuroimage* **31**, 968–980 (2006).
27. Rubinov, M. & Sporns, O. Complex network measures of brain connectivity: uses and interpretations. *Neuroimage* **52,**1059–1069 (2010).
28. Glasser, M. F. et al. The minimal preprocessing pipelines for the Human Connectome Project. *Neuroimage* **80**, 105–124 (2013).
29. van Wijk, B. C. M., Stam, C. J. & Daffertshofer, A. Comparing brain networks of different size and connectivity density using graph theory. *PLoS ONE* **5**, e13701 (2010).
30. Keene, M. F. L. & Hewer, E. E. Some observations on myelination in the human central nervous system. *J. Anat.* **66**(Pt 1), 1–13 (1931).
31. Kinney, H. C., Brody, B, A., Kloman, A. S. & Gilles, F. H. Sequence of central nervous system myelination in human infancy: II. An autopsy study of myelination. *J. Neuropathol. Exp. Neurol.* **46**, 283–301 (1988).
32. Mori, S. & Zhang, J. Principles of diffusion tensor imaging and its applications to basic neuroscience research. *Neuron* **51**, 527–539 (2006).
33. Dubois, J. et al. Asynchrony of the early maturation of white matter bundles in healthy infants: quantitative landmarks revealed noninvasively by diffusion tensor imaging. *Hum. Brain Mapp.* **29**, 14–27 (2008).
34. Dubois, J. et al. Mapping the early cortical folding process in the preterm newborn brain. *Cereb. Cortex* **18**, 1444–1454 (2008).
35. Ball, G. et al. The influence of preterm birth on the developing thalamocortical connectome. *Cortex* **49**, 1711–1721 (2013).
36. van der Aa, N. E. et al. Quantification of white matter injury following neonatal stroke with serial DTI. *Pediatr. Res.* **73**, 756–762 (2013).
37. Dimitropoulos, A. et al. Brain injury and development in newborns with critical congenital heart disease. *Neurology* **81**, 241–248 (2013).
38. Lefevre J., et al. Are developmental trajectories of cortical folding comparable between cross-sectional datasets of fetuses and preterm newborns? *Cereb. Cortex* 1–13 (2015). http://www.cercor.oxfordjournals.org/cgi/ https://doi.org/10.1093/cercor/bhv123
39. Thomason, M. E., et al. Weak functional connectivity in the human fetal brain prior to preterm birth. *Nat. Publ. Gr.* 1–10 (2017). https://doi.org/10.1038/srep39286
40. Duerden, E. G. et al. Midazolam dose correlates with abnormal hippocampal growth and neurodevelopmental outcome in preterm infants. *Ann. Neurol.* **79**, 548–559 (2016).
41. Benders, M. J., et al. Early brain activity relates to subsequent brain growth in premature infants. *Cereb. Cortex* **9**, 1–11 (2014).